Published in final edited form as:
Dev Dyn. 2014 September ; 243(9): 1116–1129. doi:10.1002/dvdy.24158.

Mammalian *Nkx2.2*+ Perineurial Glia Are Essential for Motor Nerve Development

Jessica K. Clark[1], **Ashley O'keefe**[1], **Teresa L Mastracci**[2], **Lori Sussel**[2], **Michael P. Matise**[3], and **Sarah Kucenas**[1,*]

[1]Department of Biology, University of Virginia, Charlottesville, Virginia

[2]Department of Genetics and Development, Columbia University, New York, New York

[3]Department of Neuroscience and Cell Biology, Rutgers-Robert Wood Johnson Medical School, University of Medicine and Dentistry of New Jersey, Piscataway, New Jersey

Abstract

Background—All vertebrate peripheral nerves connect the central nervous system (CNS) with targets in the periphery and are composed of axons, layers of ensheathing glia and connective tissue. Although the structure of these conduits is well established, very little is known about the origin and developmental roles of some of their elements. One understudied component, the perineurium, ensheaths nerve fascicles and is a component of the blood-nerve-barrier. In zebrafish, the motor nerve perineurium is composed of CNS-derived *nkx2.2a*$^+$ perineurial glia, which establish the motor exit point (MEP) during development. To determine if mouse perineurial cells also originate within the CNS and perform a similar function, we created a *Nkx2.2:EGFP* transgenic reporter line.

Results—In conjunction with RNA expression analysis and antibody labeling, we observed *Nkx2.2*$^+$ cells along peripheral motor nerves at all stages of development and in adult tissue. Additionally, in mice lacking *Nkx2.2*, we demonstrate that *Nkx2.2*$^+$ perineurial glia are essential for motor nerve development and Schwann cell differentiation.

Conclusions—Our studies reveal that a subset of mouse perineurial cells are CNS-derived, express *Nkx2.2*, and are essential for motor nerve development. This work highlights an under-appreciated but essential contribution of CNS-derived cells to the development of the mammalian peripheral nervous system (PNS).

Keywords

perineurial glia; perineurium; motor nerve; Schwann cell; peripheral nervous system; perisynaptic Schwann cell

*Correspondence to: Sarah Kucenas, Department of Biology, Physical & Life Sciences Building, Rm 312, PO Box 400328, University of Virginia, Charlottesville, VA 22904-4328. sk4ub@virginia.edu.

Introduction

The ability of an organism to interact with its environment, reproduce and survive is dependent on the formation and health of its peripheral nerves, which connect targets in the periphery, such as muscle, to the central nervous system (CNS). Although previous studies have demonstrated that interactions between peripheral nerve components are essential for nerve assembly, the origins of some of these cell populations are still unknown (Binari et al., 2013; Jessen and Mirsky, 2005; Kucenas et al., 2008, 2009; Parmantier et al., 1999; Shantha and Bourne, 1968).

All peripheral nerves are composed of five main components: axons, Schwann cells, the endoneurium, the perineurium, and the epineurium (Kaplan et al., 2009). Previous fate-mapping studies in mice directly demonstrate that endoneurial fibroblasts and Schwann cells are neural crest-derived (Joseph et al., 2004). In contrast, studies elucidating the origin of the perineurium in mice have been less conclusive. However, reports using other model organisms describe CNS-derived peripheral glial populations that encase peripheral motor nerves (Klambt and Goodman, 1991; Kucenas et al., 2008; Lunn et al., 1987; Parker and Auld, 2006; Schmidt et al., 1997; Sepp et al., 2001, 2000). In *Drosophila*, CNS-derived glial cells are known to make up the inner and outer layers of peripheral motor nerves (Klambt and Goodman, 1991; Parker and Auld, 2006; Schmidt et al., 1997; Sepp et al., 2000, 2001). Recently, we also demonstrated in zebrafish that *nkx2.2a*$^{+}$ cells derived from the lateral floorplate of the spinal cord give rise to perineurial glial cells that migrate into the periphery and ensheath motor axons into fascicles, ultimately forming the mature motor nerve perineurium (Kucenas et al., 2008). However, in mammals, the origin of the perineurium is less clear.

In mice, three embryonic origins for this nerve component have been postulated: the neural crest, the mesoderm, and the neural tube. In an elegant study using Wnt1-Cre^{+} loxpRosa^{+} mice to fate map the contribution of the neural crest to peripheral nerves, most endoneurial and Schwann cells were found to be neural crest-derived, while perineurial cells were not (Joseph et al., 2004). Another study using in vitro cell culture, hypothesized that the perineurium was derived from the mesoderm, as fibroblasts cultured with Schwann cells and sensory neurons formed a perineurial-like sheath (Bunge et al., 1989). However, unlike perineurial cells, which express basement membrane-specific genes and form a double basal lamina, the fibroblasts in these studies had neither characteristic (Bunge et al., 1989; Jaakkola et al., 1989; Peltonen et al., 2013). Because perineurial cells are not neural crest-derived (Joseph et al., 2004) and appear to be distinct from mesodermally-derived fibroblasts (Shanthaveerappa and Bourne, 1962), we hypothesize that mammalian perineurial cells, like zebrafish perineurial cells, are derived from *Nkx2.2*$^{+}$ precursors in the spinal cord.

To investigate this hypothesis, we created a *Nkx2.2:EGFP* transgenic reporter mouse line using a modified bacterial artificial chromosome (BAC), which was created by GENSAT and deposited at Children's Hospital Oakland Research Institute (CHORI). Combining this line with RNA expression analysis and antibody labeling, we show that a subset of mouse spinal motor nerve perineurial cells express *Nkx2.2*, are CNS-derived and express perisynaptic Schwann cell (PSC) markers near neuromuscular junctions (NMJ). To test the

role of these CNS-derived perineurial glia during motor nerve development, we utilized mice conditionally lacking *Nkx2.2* (Lei et al., 2006; Mastracci et al., 2013). In these mice, we observed axon fasciculation defects and ectopic motor neurons outside of the spinal cord. Loss of *Nkx2.2* also led to a significant reduction in myelination along motor nerves as well as general nerve ultrastructural deformities and NMJ defects. In contrast, purely sensory nerves, which were not ensheathed by *Nkx2.2*$^+$ perineurial cells, were indistinguishable from control mice. Taken together, our studies demonstrate that: (1) a subset of perineurial cells in mice originate in the ventral spinal cord and express *Nkx2.2*, (2) *Nkx2.2* may be a novel marker for PSCs, and (3) *Nkx2.2*$^+$ cells play an essential role in motor nerve development, similar to what we have previously shown in zebrafish (Kucenas et al., 2008).

Results

A Subset of Mouse Perineurial Cells Express *Nkx2.2* and Are CNS-Derived

In zebrafish, the mature motor nerve perineurium is composed of *nkx2.2a*$^+$ perineurial glial cells that arise from the lateral floor-plate (p3 domain) of the spinal cord, migrate into the periphery and ensheath motor axons into nerve fascicles (Kucenas et al., 2008). Therefore, we hypothesize that the cells that make up the motor nerve perineurium in mice also arise from *Nkx2.2*$^+$ precursors in the neural tube. To investigate this hypothesis, we carefully examined peripheral Nkx2.2 mRNA and protein expression patterns during motor nerve development. At 17.5 days post coitum (E17.5), in situ hybridization with a riboprobe specific to *Nkx2.2* (Briscoe et al., 1999; Desai et al., 2008; Sussel et al., 1998) demonstrated that this transcription factor was expressed in previously reported tissue, including the ventral spinal cord, the pancreas, and the intestines (Fig. 1A and data not shown). In addition, at this same stage, we also observed *Nkx2.2* expressing cells along the motor root close to the ventral spinal cord (Fig. 1A) and within somatic muscle (Fig. 1B).

To confirm these findings, we labeled tissue with an antibody specific to Nkx2.2 and observed Nkx2.2$^+$ cells in the spinal cord, pancreas, and intestines, as has previously been described (data not shown) (Briscoe et al., 1999; Desai et al., 2008; Sussel et al., 1998). In a pattern consistent with our RNA expression analysis, we also observed Nkx2.2$^+$ cells along the developing motor nerve root at E17.5 (data not shown). To determine if these Nkx2.2$^+$ cells were migrating from the spinal cord, we labeled E17.5 embryos with an antibody to laminin in order to delineate the boundary between the spinal cord and periphery (Fig. 1C). In these studies, we observed Nkx2.2$^+$ cell bodies breaching the laminin boundary only at the motor exit point (MEP) and interpret these findings to mean that at least some peripheral Nkx2.2$^+$ cells originate within the spinal cord, similar to what has previously been described in zebrafish (Fig. 1C) (Kucenas et al., 2008). When we looked further distally along motor nerves in the periphery at E17.5, we observed Nkx2.2$^+$ cells surrounding S100$^+$ Schwann cells in a position consistent with the perineurium (Fig. 1D). To confirm that the Nkx2.2$^+$ cells observed along motor nerves were perineurial, we used an antibody specific to podoplanin (8.1.1), a well-established marker of the perineurium in mice (Schacht et al., 2005). At E17.5, all Nkx2.2$^+$ cells around the outer edge of motor nerves co-localized with 8.1.1, demonstrating these cells were indeed perineurial (Fig. 1E). However, we also observed 8.1.1 labeling that did not appear to be associated with Nkx2.2$^+$ cells (Fig. 1E). We

also occasionally observed Nkx2.2$^+$ cell bodies within the interior of the nerve, closely associated with S100$^+$ Schwann cells (Fig. 1E).

To determine if Nkx2.2$^+$ perineurial cells remained associated with motor nerves past development, we looked for their presence in juvenile animals. Similar to what we observed in zebrafish, motor nerve-associated Nkx2.2$^+$ cells persisted into adulthood, as we detected Nkx2.2$^+$ cells around the perimeter of a P21 sciatic nerve fascicle labeled with an antibody to myelin basic protein (MBP) to visualize Schwann cells (Fig. 1F). Although we also detected patchy Nkx2.2 antibody expression within the endoneurium at this stage, this labeling was background and we did not see this expression in our RNA expression analyses or transgenic reporter line. Finally, we also observed Nkx2.2 expression in individual cells dispersed in the striated muscle at P21 (Fig. 1G), which was consistent with our *Nkx.2.2* RNA expression (Fig. 1B). Taken together, we conclude that: (1) Nkx2.2 mRNA and protein expression along the motor nerve in the mouse is similar to what has previously been described in zebrafish, (2) spinal motor nerve-associated Nkx2.2$^+$ cells originate within the CNS, and (3) Nkx2.2 is a novel marker of mammalian perineurial cells.

In order to more directly study the origin and role of Nkx2.2$^+$ cells in motor nerve development, we created a *Nkx2.2:EGFP* transgenic reporter line using a BAC (RP23–224O8) that was originally created by GENSAT and deposited at CHORI. This BAC was modified such that 5′ *Nkx2.2* regulatory sequences were fused to the coding sequence for EGFP.

Before using this transgenic line to study the origin and role of perineurial cells in motor nerve development, the expression of the transgene was confirmed by examining EGFP$^+$ embryos and comparing known Nkx2.2 expression with the pattern of the reporter line. Because the transgene faithfully recapitulated endogenous Nkx2.2 expression in the spinal cord, intestines and pancreas (Fig. 2A–D) (Briscoe at al., 1999; Desai et al., 2008; Shimamura et al., 1995; Sussel et al., 1998), we proceeded to use it to study mammalian perineurial cells.

To confirm our previous data demonstrating that Nkx2.2$^+$ cells originate within the ventral spinal cord (Fig. 1C), we fixed *Nkx2.2:EGFP* embryos at various stages of motor nerve development and labeled them with antibodies specific to axons (α-tubulin) and GFP. In E8.5 *Nkx2.2:EGFP* embryos, EGFP expression was only observed in the p3 domain of the spinal cord (Fig. 2A), which is in agreement with previously described *Nkx2.2* expression (Shimamura et al., 1995). By E10.5, thin *Nkx2.2*$^+$ processes were found just outside of the spinal cord at iterated positions along the anterior-posterior axis of the embryo consistent with the spacing of motor nerves (Fig. 2B). Similar *nkx2.2a*$^+$ processes were also observed during motor nerve development in zebrafish (Kucenas et al., 2008). At E15.5, we began to observe *Nkx2.2*$^+$ cell bodies tightly associated with α-tubulin$^+$ motor axons in the periphery and by P1, when motor axons have formed neuromuscular junctions (NMJ), we observed several *Nkx2.2*$^+$ cell bodies ensheathing motor nerves as far distally as the NMJ (Fig. 2F). This progressive association and ensheathment of motor nerves is very similar to what we previously described for CNS-derived *nkx2.2a*$^+$ perineurial glia in zebrafish (Kucenas et al.,

2008) and is consistent with the hypothesis that mammalian *Nkx2.2*$^{+}$ perineurial cells are also CNS-derived.

To confirm our earlier antibody data (Fig. 1) illustrating that Nkx2.2^{+} cells are a component of the motor nerve perineurium, we labeled *Nkx2.2:EGFP* mice with a well-established perineurial marker, zona occludins 1 (ZO-1), which is considered a hallmark of perineurial differentiation (Kristensson and Olsson, 1971; Pummi et al., 2004). In longitudinal sections at the level of the spinal motor nerve at E17.5, we observed low levels of ZO-1 immunoreactivity in GFP^{+} cells associated with S100^{+} motor nerves (data not shown). In adult sciatic nerves also sectioned longitudinally, we observed significantly higher levels of ZO-1 labeling within GFP^{+} perineurial layers around the perimeter of the nerve (Fig. 2G). Finally, to confirm these findings, we used an antibody to 8.1.1, a well-established marker of the perineurium, on adult sciatic nerve and observed 8.1.1 expression spanning the perineurial component of the nerve (Fig. 2H). Taken together, these data led us to conclude that a subset of mammalian perineurial cells express *Nkx2.2*, are CNS-derived, and ultimately form the mature motor nerve perineurium.

To independently confirm these data, we used lineage tracing with a transgenic line in which a *Nkx2.2* p3 cis-regulatory module drives Cre recombinase (Lei et al., 2006). Using both *Nkx2.2*^{Cre}*;lacZ*^{flox} and *Nkx2.2*^{Cre}*;Tomato*^{flox} reporter lines (Madisen et al., 2009; Soriano, 1999), we examined *Nkx2.2* expression along peripheral motor nerves during development. Similar to what we observed in *Nkx2.2:EGFP* embryos, β-galactosidase (β-gal) expression in *Nkx2.2*^{Cre}*;lacZ*^{flox} embryos was restricted to the p3 domain of the spinal cord at E9.5 (Fig. 3A). At E11.5, we observed β-gal^{+} projections just outside of the spinal cord at iterated positions along the anterior-posterior axis of the embryo, and by E18.5 we detected β-gal^{+} cell bodies along motor nerves in positions consistent with cells of the perineurium (Fig. 3B, C). To verify the expression of *Nkx2.2* in cell bodies, we used the *Nkx2.2*^{Cre}*;Tomato*^{flox} reporter line in conjunction with a α-tubulin antibody to label axons. Because *Nkx2.2* is transiently expressed prior to neurogenesis (Wang et al., 2011), we also observed *Nkx2.2*$^{+}$ motor axons in these studies (Fig. 3D – F). However, we never observed Islet-1/2^{+} motor neuron cell bodies outside of the spinal cord in wild-type embryos (data not shown). Identical to the expression observed in the *Nkx2.2*^{Cre}*;lacZ*^{flox} line, we observed a small number of *Nkx2.2*$^{+}$ cell bodies at the MEP just ventral to the spinal cord at E12.5 (Fig. 3D). By E15.5, several more *Nkx2.2*$^{+}$ cells were associated with the peripheral motor nerve and were located at more distal locations than seen at E12.5 (Fig. 3E). Ultimately, at E18.5, we saw many *Nkx2.2*$^{+}$ cell bodies along motor nerves (Fig. 3F). Taken together, our *Nkx2.2:EGFP* line faithfully recapitulates endogenous *Nkx2.2* expression and we conclude that a subset of mouse perineurial cells are CNS-derived and express *Nkx2.2*, similar to what has previously been described in zebrafish (Kucenas et al., 2008).

Cells at the NMJ Express *Nkx2.2*

During the course of our studies, we observed *Nkx2.2*$^{+}$ cells not only forming the motor nerve perineurium (Fig. 2E–H), but also dispersed within striated muscle in a pattern reminiscent of NMJs (Fig. 1B,G). To determine if these *Nkx2.2*$^{+}$ cells were close to the NMJ and their associated perisynaptic Schwann cells (PSC), we labeled sections taken from the

trunk region of E15.5 and E17.5 *Nkx2.2:EGFP* mice with S100, which is considered a PSC marker (Georgiou and Chalton, 1999; Woolf et al., 1992). Beginning at E15.5, a stage when PSCs are found loosely associated with developing NMJs, all $S100^+$ cells in the muscle were *Nkx2.2*$^-$ (Fig. 4A–A”). However, just two days later at E17.5, 100% of the $S100^+$ cells we observed in the muscle were also *Nkx2.2*$^+$ (Fig. 4B–B”). These data could mean that either *Nkx2.2* is turned on after E15.5 in the PSCs at the NMJ, or that *Nkx2.2*$^+$/$S100^+$ cells do not arrive at the nerve terminals until E17.5. Either is consistent with *Nkx2.2* labeling $S100^+$ cells that have previously been described as PSCs at E17.5 (Georgiou and Charlton, 1999; Woolf et al., 1992).

To further investigate these *Nkx2.2*$^+$/$S100^+$ cells, we labeled embryos with other known markers of NMJs and their associated PSCs, including α-bungarotoxin, synaptophysin, and myelin protein zero (P0) (Georgiou and Charlton, 1999; Wiedenmann and Franke, 1985). At E17.5, we observed *Nkx2.2*$^+$/S100+ cells closely opposed to NMJs as determined by α-bungarotoxin labeling (Fig. 4B–B”). One hundred percent of these *Nkx2.2*$^+$ cells at the NMJ were also $P0^+$ (data not shown). Interestingly, *Nkx2.2*$^+$ cells observed along the nerve trunk (as determined by α-tubulin labeling) prior to it branching into smaller nerve fascicles in the muscle rarely expressed P0 or any other PSC marker (data not shown). Additionally, *Nkx2.2*$^+$ cells found juxtaposed to nerve terminals were tightly associated with the synaptic vesicle marker, synaptophysin (Fig. 4C–C”). Therefore, we hypothesize that *Nkx2.2* labels two distinct glial populations: the population of perineurial glia found along nerve trunks that form the motor nerve perineurium and a second population that is found at NMJs with molecular characteristics similar to PSCs.

Towards the end of the embryonic period, around E17.5, we noticed that *Nkx2.2*$^+$/$S100^+$ cellular debris began to accumulate around the NMJ (Fig. 4D). At P1, caspase, an active enzyme in apoptotic cells, was found in close apposition to these *Nkx2.2*$^+$/ $S100^+$ cells in a pattern consistent with AChR expression (Fig. 4E). Because nerve terminal input withdrawal occurs within the first two postnatal weeks, we hypothesize that the debris we observed may be from synapse elimination (Balice-Gordon et al., 1993; Wang et al., 2014). To determine if these *Nkx2.2*+/$S100^+$ cells persist past synapse elimination and are a component of the mature NMJ, we labeled muscle tissue at P1 and adult (>P60) stages to document the relationship of the *Nkx2.2*$^+$/$S100^+$ cells and α-bungarotoxin$^+$ NMJs. Between P1 and adulthood, we observed maturation of NMJs (as determined by α-bungarotoxin labeling) and associated *Nkx2.2*$^+$/$S100^+$ glia changed morphologically to mirror the NMJ structure (Fig. 4F,G). These data raise the intriguing possibility that *Nkx2.2*$^+$ cells found at NMJs may be distinct from those found along motor nerves and that *Nkx2.2*$^+$ cells may play an active role in synapse elimination and maturation.

Loss of *Nkx2.2*$^+$ Disrupts Motor Nerve Development

Thus far, we present data that illustrates that a subset of spinal motor nerve-associated perineurial cells in mouse are CNS-derived and express *Nkx2.2*. In zebrafish, we have previously demonstrated that the loss of perineurial glia leads to motor axon pathfinding defects and ectopic motor neuron migration out of the spinal cord (Kucenas et al., 2008, 2009). To determine if mammalian *Nkx2.2*$^+$ perineurial glia play a similar role in motor

nerve assembly, we assayed motor nerve development in a conditional null allele of the *Nkx2.2* gene (*Nkx2.2*$^{flox/flox}$ cKO) using a *Nkx2.2*-specific Cre recombinase (Lei et al., 2006; Mastracci et al., 2013). This *Nkx2.2*-specific Cre is under the transcriptional control of a *Nkx2.2* cis-regulatory element that does not drive expression in the pancreas. This prevents the hyperglycemia-induced perinatal lethality observed in mice homozygous for a null mutation of *Nkx2.2* allowing us to observe the phenotype brought about by the loss of *Nkx2.2* into adulthood.

Following the loss of *Nkx2.2* (*Nkx2.2*$^{flox/flox}$ cKO), tubulin+ motor axons in the PNS were defasciculated compared to control littermates at E12.5 (Fig. 5A,C) and exited the spinal cord in ectopic locations (data not shown) (n=4(WT), 3(cKO)). Additionally, we observed Islet-1/2^{+} motor neuron cell bodies outside of the spinal cord along the peripheral nerve at E15.5 in *Nkx2.2*$^{flox/flox}$ cKOs, which we never observed in wild-type or heterozygous littermates (Fig. 5B,D) (n=4(WT), 5(cKO)). These motor nerve defects were very similar to what we previously observed in zebrafish lacking perineurial glia (Kucenas et al., 2008). From these data, we conclude that loss of *Nkx2.2* perturbs perineurial development, which in turn, leads to severe motor nerve perturbations.

To more closely investigate the perineurial defects, we used transmission electron microscopy (TEM) on adult sciatic nerves harvested from *Nkx2.2*$^{flox/flox}$ cKOs and littermate controls (n=4(WT), 4(cKO)). In wild-type littermates, the perineurium was a tightly packed series of perineurial cell layers that were easily distinguishable by the presence of double basal lamina (Fig. 6A,C). In contrast, in *Nkx2.2*$^{flox/flox}$ cKOs, the perineurium was severely deformed (Fig. 6B,D). We could not identify individual layers of perineurial cells and often observed physical deformities in the perineurial layers that appeared as if the cells were folding out away from the nerve interior instead of tightly encasing it (Fig. 6D). In these aberrantly folded perineurial layers, we also failed to visualize the double basal lamina that are a hallmark of the perineurium, which is consistent with the hypothesis that in animals lacking *Nkx2.2*, perineurial cells fail to differentiate (Fig. 6D). In support of this hypothesis, unlike perineurial cells in control littermates, perineurial glial cell bodies were not elongated in *Nkx2.2*$^{flox/flox}$ cKO animals (Fig. 6A,B). Instead, they were still round and immature.

During the course of our analysis of the TEM images we collected in control and *Nkx2.2*$^{flox/flox}$ cKO adults, we noticed that in general, the perineurium was significantly thinner around the perimeter of the sciatic nerve (data not shown). To better observe and quantify this observation, we sectioned sciatic nerves from adult animals and labeled them with antibodies specific to ZO-1 and MBP to label the mature perineurium and myelinated axons, respectively. In control sciatic nerves, ZO-1 labeling was consistent around the entire perimeter of the sciatic nerve and measured on average 65 μm (Fig. 6E, G) (n=4(WT)). In contrast, in *Nkx2.2*$^{flox/flox}$ cKOs, ZO-1 immunoreactivity was inconsistent around the perimeter of the sciatic nerve and measured on average, only approximately 30 μm (Fig. 6F, G) (n=4(cKO)). Additionally, the ZO-1 immunoreactivity in these animals also labeled aberrant structures that strikingly resembled the highly folded layers of perineurial cells we observed in TEM (Fig. 6D). We also noticed that in control littermates, the ZO-l labeling spanned the entire perineurial thickness and ended at the interface of the interior of the nerve (Fig. 6E). In contrast, in *Nkx2.2*$^{flox/flox}$ cKO nerves, ZO-1 immunoreactivity only labeled the

most peripheral portion of the perineurial compartment (Fig. 6F). However, the innermost layers of the perineurium were populated by cells as evidenced by the presence of TO-PRO$^+$ nuclei (Fig. 6F). This data, in conjunction with our earlier data demonstrating that not all perineurial cells express Nkx2.2 (Fig. 1E), is consistent with the hypothesis that the mammalian perineurium might be derived from two independent sources, and in mice lacking *Nkx2.2* the inner perineurial epithelium is affected.

Perturbed Perineurial Development Affects Schwann Cell Development and NMJ Maturation

In zebrafish, failure of perineurial glial differentiation adversely affects Schwann cell development (Kucenas et al., 2008, Binari et al., 2013). To determine if perineurial–Schwann cell interactions are also important during mammalian spinal motor nerve development, we investigated Schwann cell differentiation in adult *Nkx2.2$^{flox/flox}$* cKO mice. Using sciatic nerves, we investigated myelination by labeling tissue sections with an antibody specific to MBP as well as using TEM to assay myelin ultrastructure. In contrast to control littermates, *Nkx2.2$^{flox/flox}$* cKO mice had severely perturbed myelination around axons (Fig. 7A,C) (n=4(WT), 4(cKO)). Although each large diameter axon within the nerve was ensheathed by myelin in mutant nerves, the myelin was not compact and we often observed “swirls” within the myelin layers (Fig. 7C). We confirmed these findings in MBP-labeled tissue sections and we observed MBP immunoreactivity was less concentrated in animals lacking *Nkx2.2* (Fig. 7B, D). From these data, we conclude that conditional deletion of *Nkx2.2* perturbs perineurial differentiation, which in turn, affects Schwann cell differentiation.

In addition to the perineurial labeling we observed in our *Nkx2.2:EGFP* transgenic line, we also observed cells at the NMJ that were GFP$^+$ (Fig. 4). To determine if these cells played a role in NMJ development and maturation, we investigated NMJs in *Nkx2.2$^{flox/flox}$* cKO mice. In adult somatic muscle sections labeled with an antibody specific to α-bungarotoxin, we assayed the number and size of NMJs. Compared to wild-type littermates, NMJs in *Nkx2.2$^{flox/flox}$* cKOs were more numerous and significantly larger (Fig. 8A–D) (n=4(WT), 3(cKO)), which is consistent with our hypothesis that *Nkx2.2$^+$* cells at the NMJ are important for NMJ maturation.

Discussion

The perineurium is a critical peripheral nerve component responsible for ensheathing and protecting axons from environmental insult. Although the importance of the mature perineurium is not debated, its origin has been for many years, and the paucity of perineurial cell specific markers has made tracing its origin very difficult (Bunge et al., 1989; Joseph et al., 2004; Kucenas et al., 2008). Here, our results describe the characterization of Nkx2.2 expression in the PNS of mice using three distinct lines in combination with immunohistochemistry and in situ hybridization. As previously described in zebrafish, we found Nkx2.2 expression in a subset of CNS-derived perineurial cells that ensheath the developing and mature motor nerve. Interestingly, Nkx2.2 was also expressed in cells near the NMJ, raising the possibility that Nkx2.2 may be a novel molecular marker of PSCs or

represent another distinct population of synaptic glia. Finally, using mice with a conditional null allele of the *Nkx2.2* gene, we observed motor nerve formation defects, similar to those observed in zebrafish, including ectopic motor neuron migration from the spinal cord, myelination defects, and failure of NMJ maturation, demonstrating that $Nkx2.2^{+}$ perineurial glia are necessary for the development of peripheral spinal motor nerves.

Up until now, the developmental origin of the perineurium has been controversial. In vitro experiments suggested that the perineurium was derived from the mesoderm, as cranial periosteal fibroblasts form a perineurial-like sheath when co-cultured with Schwann cells and sensory neurons (Bunge et al., 1989). However, in vivo, perineurial cells express basement membrane-specific genes (*α1(I)* and *α2(IV) collagen* and *laminin B2 chain*) and form a basement membrane that sets them apart from fibroblasts (Jaakkola et al., 1989; Peltonen et al., 1987). Furthermore, electron microscopy differentiates fibroblasts and perineurial cells as distinct entities. Fibroblast cells have more compact nuclei and their endoplasmic reticulum is more obvious than that observed in perineurial cells (Shantha and Bourne, 1968).

An attractive theory was postulated by Shantha and Bourne (1968) in which they believe there are two components to the perineurium: an epithelium that is composed of a number of squamous cell layers that surround the nerve fascicle and a more peripheral connective tissue that is juxtaposed to the epineurium. Hematoxylin-eosin staining shows these differences between the two layers as the connective tissue stains less intensely than the epithelial layer (Shantha and Bourne, 1968). Interestingly, electron microscopy has shown that the dura matter of the spinal cord continues into the periphery as the connective tissue and the epineurium, while the pia-arachnoid layers (or leptomeninges) continue as the epithelium (Shantha and Bourne, 1968). Shanthaveerappa and Bourne claim that the epithelium is so morphologically and histochemically identical to the cells that make up the pia-arachnoid layer, that these structures must share an origin, namely the neuroectoderm (Shanthaveerappa and Bourne, 1962). This suggests that perhaps the reason that the origin of the perineurium has been so highly debated is because the perineurium has two distinct components derived from distinct progenitors. If this epithelial layer was indeed ectodermal, it would suggest that the origin is neural tube, as lineage tracing has determined that the perineurium is not neural crest-derived (Joseph et al., 2004). This would be consistent with other studies that have shown that the perineurium, or analogous structures, are derived from the CNS in zebrafish and in *Drosophila* (Klambt and Goodman, 1991; Kucenas et al., 2008; Parker and Auld, 2006; Schmidt et al., 1997; Sepp et al., 2000, 2001).

In agreement with this hypothesis set forth 60 years ago, our current work demonstrates that $Nkx2.2^{+}$ and $8.1.1^{+}$ labeling is not always perfectly aligned (Figs. 1E, 4C). 8.1.1 is a stromal cell line marker found not only in the perineurium but also in a number of other cell types such as myofibroblasts and myoepithelium (Schacht et al., 2005). This suggests that 8.1.1 may also be labeling fibroblasts, which may explain the divergent hypotheses on the origin of the perineurium and is consistent with the hypothesis that the perineurium could be composed of more than one cell type. Additionally, in our knock-out studies, we observe perineurial defects, as assessed by ZO-1 labeling, that demonstrate that in the absence of *Nkx2.2*, ZO-1 labeling is lost in the inner layers of the perineurium (Fig. 6H) but maintained

in the outer layers, which have been hypothesized to be a distinct connective tissue layer. Unfortunately, due to the lack of specific perineurial cell markers (beyond Nkx2.2), it is not possible to determine what percentage of perineurial cells are from the mesoderm versus ectoderm. However, future studies to determine the molecular characteristics of the non-Nkx2.2 population of perineurial cells would be beneficial to further characterize this important component of the peripheral nervous system.

In addition to motor nerve–associated Nkx2.2^{+} perineurial glia, we also observed Nkx2.2^{+} cells within the interior of developing nerve fascicles as well as near the NMJ. Whether these cells are perineurial glia or a new class of peripheral glia, and whether they are CNS-derived, remains to be seen. However, we were able to distinguish them from perineurial glia using both antibody labeling and the various transgenic constructs we use in this study. Interestingly, in mice conditionally lacking Nkx2.2, NMJs fail to mature normally (Fig. 8), leading us to conclude that Nkx2.2^{+} cells at the NMJ are essential mediators in this process and raise the intriguing hypothesis that they may also play a role in regeneration.

In conclusion, our studies demonstrate that the origin of perineurial cells is conserved between zebrafish and mice and that these cells play essential roles in nerve development. A more complete understanding of the role of perineurial glia in neural development will elucidate insights into diseases of the PNS and highlight an underappreciated role of the CNS in PNS development.

Experimental Procedures

Mouse Husbandry

Adult mice were kept in standard mouse cages under a 12:12 hr light:dark cycle with water and chow available ad libitum. Timed matings were staged based on the appearance of vaginal plugs, which was considered to be embryonic day 0.5 (E0.5). All animal procedures were approved by the University of Virginia Animal Care and Use Committee.

Generation of Mouse Lines

Nkx2.2:EGFP mice were created by standard pronuclear DNA injection methods at the University of Virginia Gene Targeting and Transgenic Facility using a modified BAC (RP23–224O8) purchased from Children's Hospital Oakland Research Institute (CHORI). To recreate the transgenic line originally made by GEN-SAT, purified BAC DNA (1 ng/μl) was microinjected into the male pronucleus of 122 fertilized oocytes from C57BL/6 mice crossed with SJL agouti mice (courtesy of the Gene Targeting and Transgenic Facility at the University of Virginia). One hundred of these zygotes were implanted into the oviduct of pseudopregnant females and genotyping occurred at the time of weaning. Non-EGFP mice were not examined further. From the 100 fertilized oocytes implanted, 3 founder mice were *Nkx2.2:EGFP*$^{+}$ and the two that survived were crossed into a C57BL6 background. The expression pattern of the two founders was identical, with founder 2 having slightly stronger expression (data not shown). Therefore, founder 2 and its progeny were bred and used for the purposes of this study. The *Nkx2.2*$^{p3\text{-}CRM}$*::Cre* mouse line has previously been reported (Lei et al., 2006), as have the *Gt*(*ROSA*)*26-Sor*^{tm1Sor}, the

Gt(ROSA)26Sor$^{tm9(CAG\text{-}tdTomato)Hze}$ reporter lines (Madisen et al., 2010; Soriano, 1999) and the conditional *Nkx2.2* allele (*Nkx2.2*$^{tm5.1Suss}$) (Mastracci et al., 2013). Mice from *Nkx2.2*$^{p3\text{-}CRM}$*::Cre x ROSA26*^{flxlz} crosses are referred to as *Nkx2.2*^{Cre}*;lacZ*^{flox} mice and mice from *Nkx2.2*$^{p3\text{-}CRM}$*::Cre x Gt(RO-SA)26Sor*^{tm1Sor} crosses are referred to as *Mx2.2*^{Cre}*;Tomato*^{flox}. Mice from *Nkx2.2*$^{p3\text{-}CRM}$*::Cre x Nkx2.2*$^{tm5.1Suss}$ crosses are referred to as *Nkx2.2*$^{flox/flox}$ cKO. The following primer sets were used for genotyping: Cre (forward: 5'-GCG GTC TGG CAG TAA AAA CTA TC-3′; reverse: 5′-GTG AAA CAG CAT TGC TGT CAC TT-3′); Rosa (1: 5′-AAA GTC GCT CTG AGT TGT TAT-3′; 2: 5′-GCG AAG AGT TTG TCC TCA ACC-3′; 3: GGA GCG GGA GAA ATG GAT ATG-3′); Tomato (forward: 5′-CTG TTC CTG TAC GGC ATG G-3′; reverse: 5′-GGC ATT AAA GCA GCG TAT CC-3′); GFP (forward: 5′-AAG TTC ATC TGC ACC ACC G-3′; reverse: 5′-TCC TTG AAG AAG ATG GTG CG-3′). *Nkx2.2*$^{tm5.1Suss}$ allele genotyping required two sets of primers: L83 (forward: 5′-TCC TTT TAA AAA TCT GCC CAC GTC T-3′), L83 (reverse: 5′-GGA TTT GGA GCT CGA GTC TTG G-3′); FL146 (forward 5′-GGG TTA TCC AGA CAG TGG AGG AGT G-30), FL146 (reverse 5′-GAG GTC AAC TAG GCC TCAA CTT GGT-3′).

Tissue Harvest

For harvesting embryos prior to E17, pregnant dams were sacrificed by CO_2 and embryos were removed and fixed in 4% paraformaldehyde. Embryos harvested after E17.5 were extracted from anesthetized pregnant dams that were deeply anesthetized with a solution of ketamine and xylazine and perfused intracardially with 5 mL of 0.1 M phosphate buffered saline (PBS) at pH 7.35, followed by 20 mL of cold 4% paraformaldehyde in 0.1 M PBS at pH 7.35. Sciatic nerves were dissected out of adult mice and post-fixed in 4% paraformaldehyde. Fixed tissue was blocked in agar and placed overnight at 4°C in 30% sucrose. Thirty-micrometer sections were collected on a cryostat microtome and were stored at − 80° C until processing.

Immunohistochemistry, DAB, and X-gal Staining

To process for immunohistochemistry (IHC), frozen sections were rehydrated for 30 min in 0.1 M PBS and rinsed 3 ×10 min in 0.1 M PBS with 0.1% Triton X-100 (PBSTx) followed by background blocking with 5% normal goat serum in PBS-Tx for 1 hr at 23° C. Sections were incubated in primary antibody in PBS-Tx with 5% normal goat serum overnight at 4° C. Primary antibodies used included mouse anti-acetylated tubulin (Sigma, St. Louis, MO; 1:5,000), rabbit anti-laminin (Sigma; 1:100), rabbit anti-S100 (Abcam, Cambridge, MA; 1:1,000), chicken anti-GFP (Aves Lab, Tigard, OR; 1:500), rabbit anti-MBP (Abcam; 1:500), rabbit anti-ZO-1 (Invitrogen, Carlsbad, CA, 1:500), Caspase-6 (BioVision, Malpitas, CA; 1:100), synaptophysin (Synaptic Systems, Goettingen, Germany; 1:1,000), Alexa Fluor 555 alpha-bungarotoxin (Molecular Probes, Eugene, OR; 1:500), TO-PRO-3 Iodide (642/661) (Invitrogen; 1:1,000), mouse anti-islet-1/2 homeobox (Developmental Studies Hybridoma Bank; 1:100), hamster anti-8.1.1 (Developmental Studies Hybridoma Bank, Indianapolis, IN; 1:25), and mouse anti-Nkx2.2 (Developmental Studies Hybridoma Bank; 1:25). The 8.1.1 (developed by A. Farr), Islet1/2 homeobox (developed by T.M. Jessell and S. Brenner-Morton), and the Nkx2.2 (developed by T.M. Jessell and S. Brenner-Morton) antibodies were obtained from the Developmental Studies Hybridoma Bank developed

under the auspices of the NICHD and maintained by The University of Iowa, Department of Biology, Iowa City, IA 52242. Sections were extensively washed with PBS-Tx, incubated with Alexa Fluor 488, Alexa Fluor 568, and/or Alexa Fluor 647 (Invitrogen) as secondary antibodies for detection of primary antibodies overnight in PBS-Tx with 5% normal goat at 4°C and washed with PBS-Tx for 3 × 10 min. Sections were mounted in Aqua Polymount (Polysciences, Warrington, PA). To process for lacZ in embryos E13 or younger, whole embryos were fixed in 4% PFA overnight at 4°C. Embryos were placed in X-Gal buffer (5 mM potassium ferrocyanide, 5 mM potassium ferricyanide, 1 mM magnesium chloride, 0.2% Triton X-100, 1 mg/ml X-Gal in PBS) and staining was performed overnight at 23° C. Embryos were dehydrated through graded washes of ethanol and were then cleared in methyl salicylate. Embryos older than E13 were cryosectioned and X-Gal staining was performed on sections. Confocal images were acquired using either a 25x or 40x multi-immersion objective (numerical aperture = 0.8 and 1.40, respectively) mounted on a motorized Zeiss AxioObserver Z1 microscope equipped with a Quorum WaveFX-X1 spinning disc confocal system (Quorum Technologies Inc., Guelph, Canada) or a 10x or 20x multi-immersion objective (numerical aperture = 0.45 and 0.75, respectively) mounted on a Zeiss AxioObserver Z1 microscope equipped with Zeiss AxioVision software. All images were imported into Adobe Photoshop. Adjustments were limited to levels, contrast, color matching settings, and cropping.

In Situ RNA Hybridization

Fixed embryos were dehydrated through graded washes of methanol and stored in 100% methanol at −20°C prior to in situ hybridization. Embryos were rehydrated through graded washes of methanol, blocked in agar and placed overnight at 4°C in 30% sucrose. Fourteen-micrometer sections were collected on a cryostat microtome and were immediately placed in 4% PFA for 15 min. Slides were washed twice (5 min) with PBS (treated with 0.1% activated DEPC) and were equilibrated for 15 min in 5x SSC. Slides were then prehybridized for 2 hr at 58°C in hybridization buffer (50% Formamide, 5X SSC, 40 μg/ml salmon sperm DNA). DIG-labeled probe (400 ng/ml) was added to hybridization buffer, denatured for 5 min at 80°C. The sections were then hybridized with the denatured digoxigenin-labeled *Nkx2.2* riboprobe (Briscoe et al., 1999; Desai et al., 2008) and placed in a humidifier box at 58° C overnight. On day 2, slides were washed in successive hot washes of hybridization buffer (2x SSC, 2x SSC, 0.1x SSC) at 65°C. Sections were equilibrated in buffer 1 (Tris 100mM/NaCl 150 mM, pH 7.5) for 5 min at 23°C, which was replaced by anti-DIG alkaline phosphatase antibody (Roche, Indianapolis, IN) diluted 1:5,000 in buffer 1 +0.5% Boehringer Blocking Reagent (Roche) and incubated for 2 hr at 23° C. Following two 15-min washes in buffer 1, slides were equilibrated for 5 min with buffer 2 (Tris 100 mM, NaCl 100 mM, $MgCl_2$ 50 mM, pH 9.5). Sections were stained in buffer 2 containing 45 μl NBT and 35 μl BCIP per 10 ml of buffer 2 until a strong signal was observed at which point the staining reaction was stopped by a wash with TE buffer (Tris 10 mM, EDTA 1 mM, pH 8.0) for 15 min. Sections were coverslipped with 80% glycerol.

Transmission Electron Microscopy

Sciatic nerves were collected from adult *Nkx2.2*$^{flox/flox}$ cKO mice and their littermates. These nerves were postfixed with fresh 4% PFA and 2.5% glutaraldehyde overnight at 4°C.

Nerves were rinsed in distilled water and incubated for 1 hr in 2% osmium tetroxide. Following the incubation, they were washed with distilled water and were dehydrated sequentially in increasing concentrations of ethanol and acetone (EM grade, Electron Microscopy Sciences, Fort Washington, PA). Nerves were then treated with 50/50 acetone/resin (EMBED812; EMS) for 2 hr, followed by full resin overnight. Nerves were then embedded in fresh 100% EPON, bake in a 65°C oven. Using a Leica Ultracut UCT, ultrathin sections were cut at 75 nm, picked up on 200-mesh copper grids, and contrast stained with 0.25% lead citrate and 2% uranyl acetate grids. Ultrathin sections were examined on a JEOL 1010 electron microscope. A 16 M pixel digital camera (SIA-12C, Scientific Instruments and Applications, Duluth, GA) was used to capture images at 4,000× or 8,000× magnification. Images were processed using ImageJ.

NMJ and Perinuerium Width Quantification

To quantify the average width of the perineurium in *Nkx2.2*$^{flox/flox}$ cKOs compared to their control littermates, approximately seven images were taken per animal (n=4(WT), 4(cKO)) and the width of the perineurium was blindly measured and logged using ImageJ. To quantify the average width of individual NMJs in *Ntec2.2*$^{flox/flox}$ cKOs compared to their control littermates, approximately nine images were taken per animal (n=4(WT), 4(cKO)) and the widths of the NMJs were blindly measured at their widest point and logged using ImageJ. To quantify the average number of NMJs in somatic muscle in *Nkx2.2*$^{flox/flox}$ cKOs compared to their control littermates, five 10 images were taken per animal (n=4(WT), 3(cKO)) and sections were blindly counted and logged using ImageJ.

Data Quantification and Statistical Analysis

Data are presented as the mean ± SEM. Data analysis was conducted using an unpaired t-test for the comparison of differences between mouse lines. Graph Pad Prism 5.0 (Graph Pad Software, Inc., San Diego, CA) was used for statistical analyses and graph preparation. Differences were considered significant when $P < 0.05$.

Acknowledgments

We thank members of the Kucenas laboratory for valuable discussions, Sarah Kempke and Dina Balderes for mouse assistance, and Babette Fuss for comments on the manuscript. We also acknowledge the Children's Hospital Oakland Research Institute (CHORI) for the BAC clone (RP23–224O8) used to create the transgenic reporter line described in this manuscript. The 8.1.1 (developed by A. Farr), Islet1/2 (developed by T.M. Jessell and S. Brenner-Morton) and Nkx2.2 (developed by T.M. Jessell and S. Brenner-Morton) antibodies were obtained from the Developmental Studies Hybridoma Bank developed under the auspices of the NICHD and maintained by The University of Iowa, Department of Biology, Iowa City, IA 52242. J.K. and S.K. designed, performed and analyzed experiments. A.O'K. assisted J.K. and T.L.M., L.S. and M.P.M. provided mouse lines. S.K. wrote the paper with J.K. This work was supported by the National Institutes of Health (NIH) grants NS072212 (S.K.), HD057015 (M.P.M.), and DK089523 (L.S.) and the Juvenile Diabetes Research Foundation (JDRF) 3–2010-791 (T.L.M.).

Grant sponsor: National Institutes of Health (NIH); Grant numbers: NS072212, HD057015, and DK089523; Grant sponsor: Juvenile Diabetes Research Foundation (JDRF); Grant number: 3-2010-791.

References

Balice-Gordon RJ, Chua CK, Nelson CC, Lichtman JW. Gradual loss of synaptic cartels precedes axon withdrawal at developing neuromuscular junctions. Neuron. 1993; 11:801–815. [PubMed: 8240805]

Binari LA, Lewis GM, Kucenas S. Perineurial glia require notch signaling during motor nerve development but not regeneration. J Neurosci. 2013; 33:4241–4252. [PubMed: 23467342]

Briscoe J, Sussel L, Serup P, Hartigan-O'Connor D, Jessell TM, Rubenstein JL, Ericson J. Homeobox gene Nkx2.2 and specification of neuronal identity by graded Sonic hedgehog signalling. Nature. 1999; 398:622–627. [PubMed: 10217145]

Bunge MB, Wood PM, Tynan LB, Bates ML, Sanes JR. Perineurium originates from fibroblasts: demonstration in vitro with a retroviral marker. Science. 1989; 243:229–231. [PubMed: 2492115]

Desai S, Loomis Z, Pugh-Bernard A, Schrunk J, Doyle MJ, Minic A, McCoy E, Sussel L. Nkx2.2 regulates cell fate choice in the enteroendocrine cell lineages of the intestine. Dev Biol. 2008; 313:58–66. [PubMed: 18022152]

Georgiou J, Charlton MP. Non-myelin-forming perisynaptic Schwann cells express protein zero and myelin-associated glycoprotein. Glia. 1999; 27:101–109. [PubMed: 10417810]

Jaakkola S, Peltonen J, Uitto JJ. Perineurial cells coexpress genes encoding interstitial collagens and basement membrane zone components. J Cell Biol. 1989; 108:1157–1163. [PubMed: 2921281]

Jessen KR, Mirsky R. The origin and development of glial cells in peripheral nerves. Nat Rev Neurosci. 2005; 6:671–682. [PubMed: 16136171]

Joseph NM, Mukouyama YS, Mosher JT, Jaegle M, Crone SA, Dormand EL, Lee KF, Meijer D, Anderson DJ, Morrison SJ. Neural crest stem cells undergo multilineage differentiation in developing peripheral nerves to generate endoneurial fibroblasts in addition to Schwann cells. Development. 2004; 131:5599–5612. [PubMed: 15496445]

Kaplan, S.; Odaci, E.; Unal, B.; Sahin, B.; Fornaro, M. International Review of Neurobiology. New York: Elsevier Inc.; 2009. Development of the peripheral nerve; p. 9-26.

Klambt C, Goodman CS. The diversity and pattern of glia during axon pathway formation in the Drosophila embryo. Glia. 1991; 4:205–213. [PubMed: 1827779]

Kristensson K, Olsson Y. The perineurium as a diffusion barrier to protein tracers. Differences between mature and immature animals. Acta Neuropathol. 1971; 17:127–138. [PubMed: 5101596]

Kucenas S, Takada N, Park H-C, Woodruff E, Broadie K, Appel B. CNS-derived glia ensheath peripheral nerves and mediate motor root development. Nat Neurosci. 2008; 11:143–151. [PubMed: 18176560]

Kucenas S, Wang W-D, Knapik EW, Appel B. A selective glial barrier at motor axon exit points prevents oligodendrocyte migration from the spinal cord. J Neurosci. 2009; 29:15187–15194. [PubMed: 19955371]

Lei Q, Jeong Y, Misra K, Li S, Zelman AK, Epstein DJ, Matise MP. Wnt signaling inhibitors regulate the transcriptional response to morphogenetic shh-gli signaling in the neural tube. Dev Cell. 2006; 11:325–337. [PubMed: 16950124]

Lunn ER, Scourfield J, Keynes RJ, Stern D. The neural tube origin of ventral root sheath cells in the chick embryo. Development. 1987; 101:247–254. [PubMed: 3446475]

Madisen L, Zwingman TA, Sunkin SM, Oh SW, Zariwala HA, Gu H, Ng LL, Palmiter RD, Hawrylycz MJ, Jones AR, Lein ES, Zeng H. A robust and high-throughput Cre reporting and characterization system for the whole mouse brain. Nat Neurosci. 2009; 13:133–140. [PubMed: 20023653]

Mastracci TL, Lin C-S, Sussel L. Generation of mice encoding a conditional allele of Nkx2.2. Transgen Res. 2013; 22:965–972.

Parker RJ, Auld VJ. Roles of glia in the Drosophila nervous system. Semin Cell Dev Biol. 2006; 17:66–77. [PubMed: 16420983]

Parmantier E, Lynn B, Lawson D, Turmaine M, Namini SS, Chakrabarti L, McMahon AP, Jessen KR, Mirsky R. Schwann cell-derived Desert hedgehog controls the development of peripheral nerve sheaths. Neuron. 1999; 23:713–724. [PubMed: 10482238]

Peltonen J, Jaakkola S, Virtanen I, Pelliniemi L. Perineurial cells in culture. An immunocytochemical and electron microscopic study. Lab Invest. 1987; 57:480–488. [PubMed: 3119943]

Peltonen S, Alanne M, Peltonen J. Barriers of the peripheral nerve. Tissue Barriers. 2013; 3:e24956. [PubMed: 24665400]

Pummi KP, Heape AM, Grenman RA, Peltonen JTK, Peltonen SA. Tight junction proteins ZO-1, occludin, and claudins in developing and adult human perineurium. J Histochem Cytochem. 2004; 52:1037–1046. [PubMed: 15258179]

Schacht V, Dadras SS, Johnson LA, Jackson DG, Hong Y-K, Detmar M. Up-regulation of the lymphatic marker podoplanin, a mucin-type transmembrane glycoprotein, in human squamous cell carcinomas and germ cell tumors. Am J Pathol. 2005; 166:913–921. [PubMed: 15743802]

Schmidt H, Rickert C, Bossing T, Vef O, Urban J, Technau GM. The embryonic central nervous system lineages of *Drosophila melanogaster*. II. Neuroblast lineages derived from the dorsal part of the neuroectoderm. Dev Biol. 1997; 189:186–204. [PubMed: 9299113]

Sepp KJ, Schulte J, Auld VJ. Developmental dynamics of peripheral glia in *Drosophila melanogaster* . Glia. 2000; 30:122–133. [PubMed: 10719354]

Sepp KJ, Schulte J, Auld VJ. Peripheral glia direct axon guidance across the CNS/PNS transition zone. Dev Biol. 2001; 238:47–63. [PubMed: 11783993]

Shantha, TR.; Bourne, GH. The structure and function of nervous tissue. New York: Academic Press; 1968. The perineural epithelium: a new concept; p. 379

Shanthaveerappa TR, Bourne GH. A perineural epithelium. J Cell Biol. 1962; 14:343–346. [PubMed: 13911261]

Shimamura K, Hartigan DJ, Martinez S, Puelles L, Rubenstein LR. Longitudinal organization of the anterior neural plate and neural tube. Development. 1995; 121:3923–3933. [PubMed: 8575293]

Soriano P. Generalized lacZ expression with the ROSA26 Cre reporter strain. Nature Genet. 1999; 21:70–71. [PubMed: 9916792]

Sussel L, Kalamaras J, Hartigan-O'Connor DJ, Meneses JJ, Pedersen RA, Rubenstein JL, German MS. Mice lacking the homeodomain transcription factor Nkx2.2 have diabetes due to arrested differentiation of pancreatic. Development. 1998; 125:2213–2221. [PubMed: 9584121]

Wang Y, Lei W, Oosterveen T, Ericson J, Matise MP. Tcf/Lef repressors differentially regulate Shh-Gli target gene activation thresholds to generate progenitor patterning in the developing CNS. Development. 2011; 138:3711–3721. [PubMed: 21775418]

Wang JY, Chen F, Fu XQ, Ding CS, Zhou L, Zhang XH, Luo ZG. Caspase-3 cleavage of dishevelled induces elimination of postsynaptic structures. Dev Cell. 2014; 128:670–684. [PubMed: 24631402]

Wiedenmann B, Franke WW. Identification and localization of synaptophysin, an integral membrane glycoprotein of Mr 38,000 characteristic of presynaptic vesicles. Cell. 1985; 41:1017–1028. [PubMed: 3924408]

Woolf CJ, Reynolds ML, Chong MS, Emson P, Irwin N, Benowitz LI. Denervation of the motor endplate results in the rapid expression by terminal Schwann cells of the growth-associated protein GAP-43. J Neurosci. 1992; 12:3999–4010. [PubMed: 1403096]

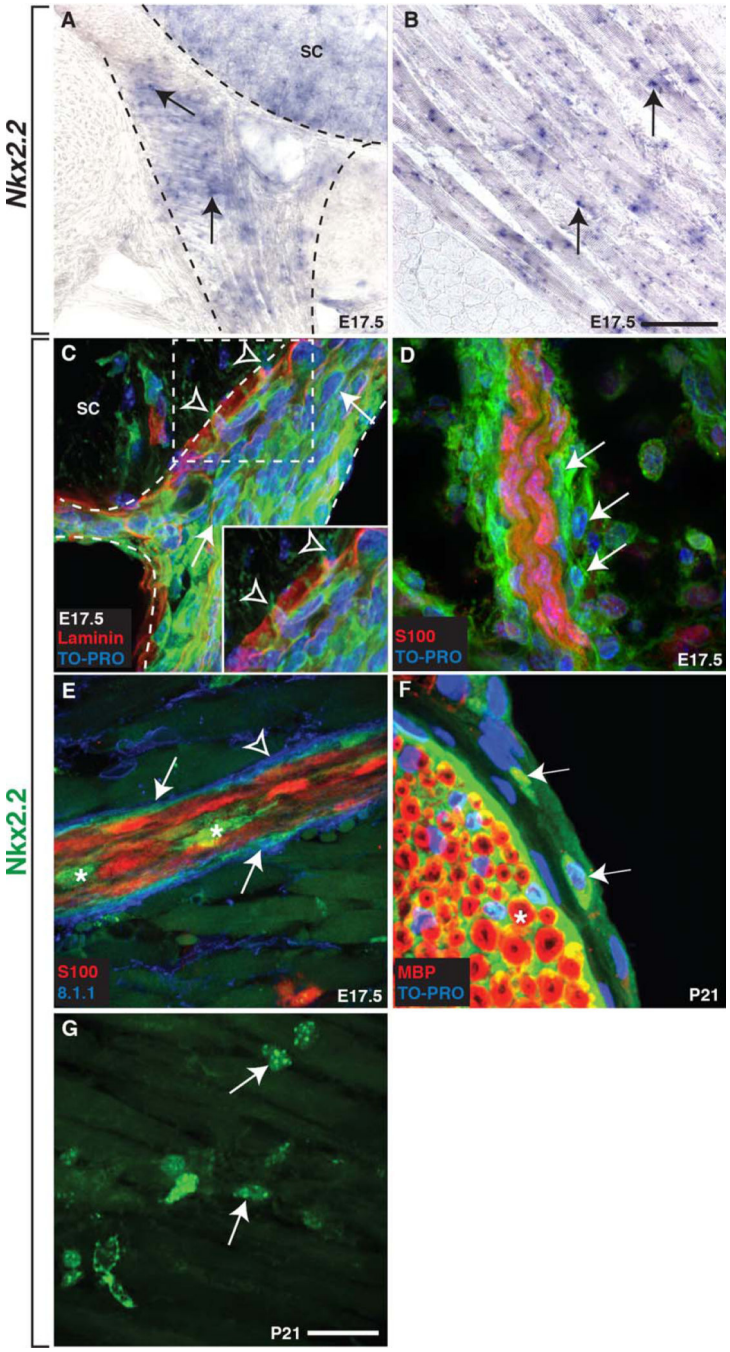

Fig. 1.

Mouse perineurial cells express Nkx2.2. **A,B**: At E17.5, *Nkx2.2* mRNA expression was detected in the (A) p3 domain of the spinal cord (sc), (A) along the developing peripheral motor nerve (arrows), and in (B) striated muscle (arrows). Dashed lines outline the spinal cord and ventral nerve. **C**: Using antibodies specific to Nkx2.2 and laminin, we confirmed this expression along motor nerves (arrow) and observed several Nkx2.2^{+} cells (open arrowheads) breaching the boundary between the CNS and PNS at the motor exit point (MEP) at E17.5. Dashed box denotes higher magnification inset of cells breaching the

CNS/PNS boundary. **D**: Further in the periphery at E17.5, we observed Nkx2.2$^+$ cells (arrows) along a motor nerve labeled with an antibody to S100 to visualize Schwann cells. **E**: Additionally, the perineurial marker 8.1.1 co-localized with Nkx2.2 (arrows) and these cells were observed ensheathing S100$^+$ Schwann cell-wrapped axons. However, not all 8.1.1 expression co-localized with Nkx2.2$^+$ cells (arrowhead). Asterisks indicate Nkx2.2$^+$ cell bodies within the nerve. **F**: At P21, Nkx2.2$^+$ (arrows) cells were observed around the perimeter of a sciatic nerve in a position consistent with the perineurium and these cells were peripheral to MBP$^+$ Schwann cells (asterisk). **G**: At P21, individual Nkx2.2$^+$ cell bodies (arrows) were also dispersed throughout the striated muscle. Black scale bar = 100 μm. White scale bar = 25 μm.

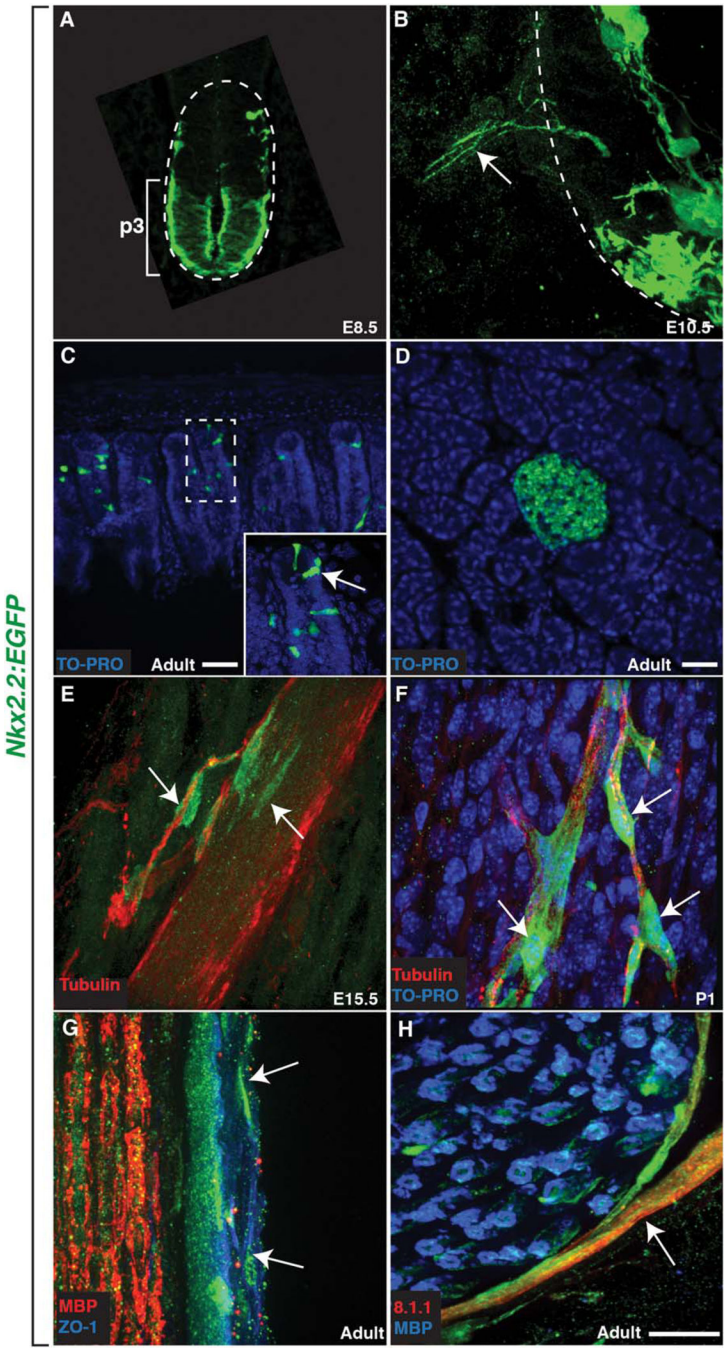

Fig. 2.

The *Nkx2.2:EGFP* transgenic reporter line recapitulates endogenous Nkx2.2 expression and labels the spinal motor nerve perineurium. **A**: EGFP expression driven by the *Nkx2.2:EGFP* transgene was restricted to the p3 domain of the spinal cord in E8.5 mice. **B**: By E10.5, *Nkx2.2*$^{+}$ processes (arrow) emerged from the spinal cord. **C,D**: Similar to previously reported expression patterns, EGFP^{+} cells were also found in the (C) intestines (arrow) and (D) pancreas. **E:** At E15.5, GFP^{+} processes were followed by *Nkx2.2*$^{+}$ cell bodies (arrows) that were tightly associated with a developing peripheral motor nerve labeled with an

antibody to tubulin. **F**: By P1, *Nkx2.2*$^{+}$ cells (arrows) ensheathed nerve fascicles well into the periphery. **G**: In adult tissue, ZO-1 labeling between *Nkx2.2:EGFP*$^{+}$ cells indicates tight junctions, a hallmark of the mature perineurium. **H**: In adult sciatic nerves, the *Nkx2.2:EGFP*$^{+}$ perineurium was also 8.1.1^{+} and *Nkx2.2:EGFP*$^{+}$ cells (arrow) were found around the perimeter of an individual nerve fascicle labeled with MBP to visualize Schwann cells. Dashed lines outline the edge of the spinal cord (A&B) and dashed box denotes magnified inset (C). Scale bars = 25 μm.

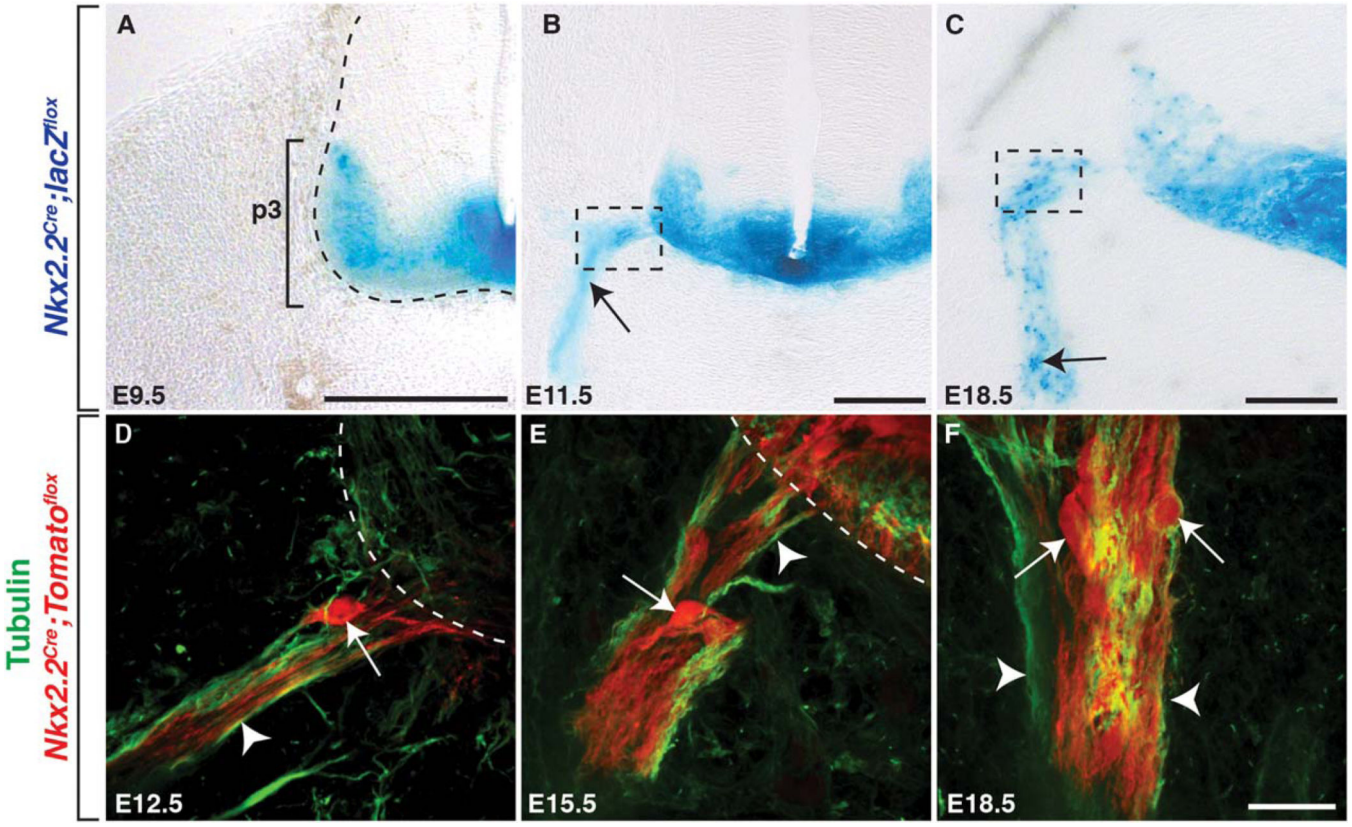

Fig. 3.

Nkx2.2^{+} perineurial cells are CNS-derived. Transverse sections of the spinal cord from *Nkx2.2*^{Cre}*;lacZ”*^{ox} mice at (A) E9.5, (B) E11.5, and (C) E18.5. **A***Nkx2.2* is constrained to the p3 domain of the ventral spinal cord at E9.5. **B:** By E11.5, we observed *Nkx2.2*$^{+}$ processes (arrow) projecting into the periphery. **C:** By 18.5, several *Nkx2.2*$^{+}$ cell bodies were observed along the peripheral motor nerve (arrow). D–F: In the *Nkx2.2*^{Cre}*;-Tomato*^{flox} line labeled with an antibody to tubulin, we observed a very similar expression profile. **D:** At E12.5, we observed a few *Nkx2.2*$^{+}$ cells (arrow) along the peripheral nerve near the MEP and by (**E**) E15.5, significantly more *Nkx2.2*$^{+}$ cells (arrow) were associated with motor axons (arrowhead) just ventral to the spinal cord. **F:** By E18.5, several *Nkx2.2*$^{+}$ cells populated the peripheral motor nerve, and these were distinct from neighboring *Nkx2.2*$^{+}$ motor axons (arrowheads). Dashed boxes in B and C indicate the approximate location that the images in D–F were taken. Dashed lines label the edge of the spinal cord. Black scale bar = 200 μm. White scale bar = 25 μm.

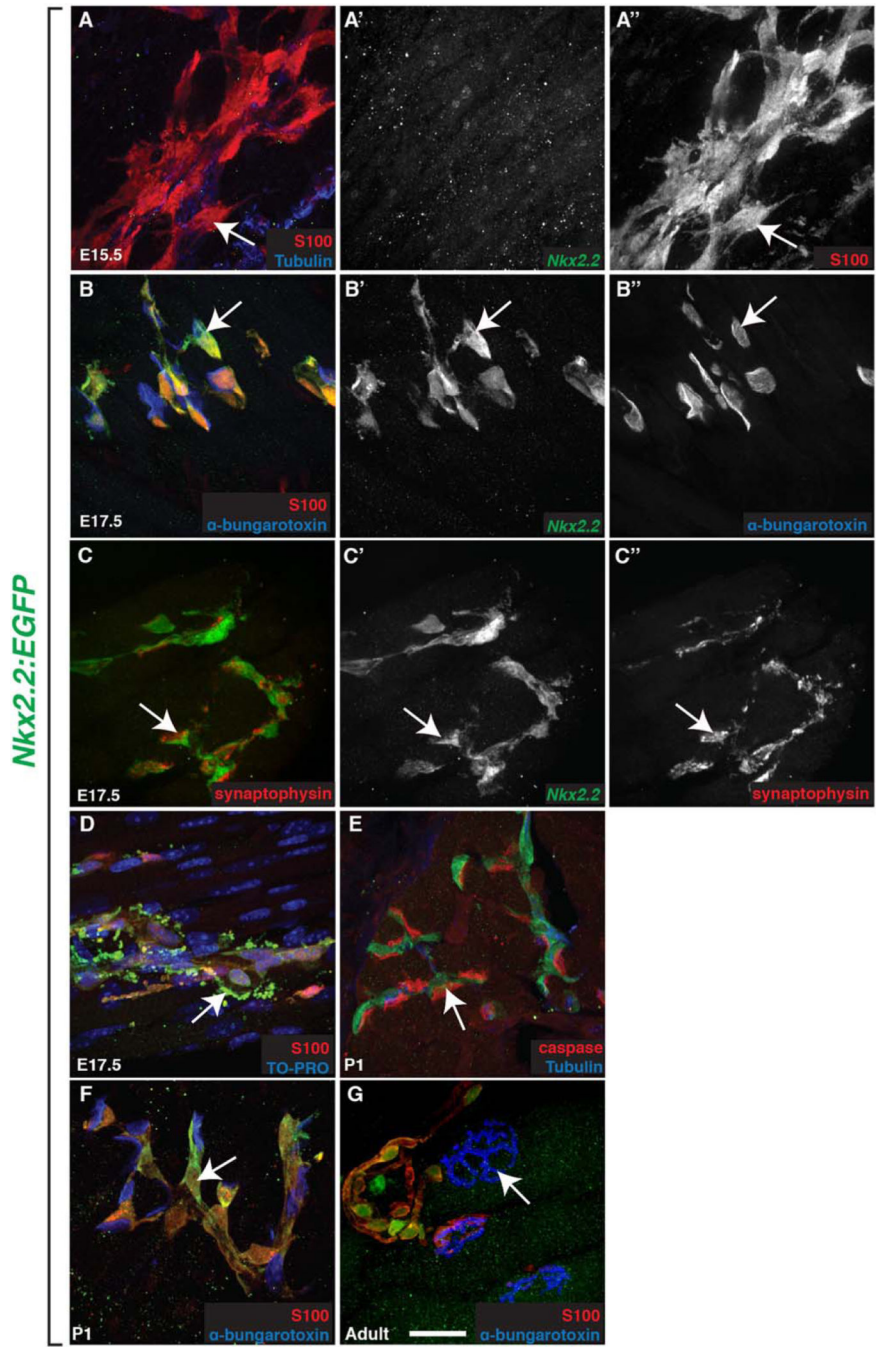

Fig. 4.

Nkx2.2^{+} cells at the NMJ express perisynaptic Schwann cell markers. **A,B:** At (B) E17.5 but not (A) E15.5, all *Nkx2.2*$^{+}$ cells (A'-B') were S100^{+} (A"; arrows) and found at α-bungarotoxin^{+} NMJs (B") within the muscle. **C:** These *Nkx2.2*$^{+}$ cells were also closely opposed to synaptophysin^{+} cells (C"; arrow) in the muscle. D: At E17.5, *Nkx2.2*$^{+}$/S100^{+} debris (arrows) was observed accumulating in the striated muscle near NMJs. E: Caspase-6 immunoreactivity was observed (arrow) at P1 near *Nkx2.2*$^{+}$ cells. **D–G**: The morphology and number of *Nkx2.2*$^{+}$/S100^{+} cells (arrows) found at α-bungarotoxin^{+} NMJs changed

during development between (B) E17.5 and (F) P1 and (G) persisted into adulthood. Scale bar = 25 μm.

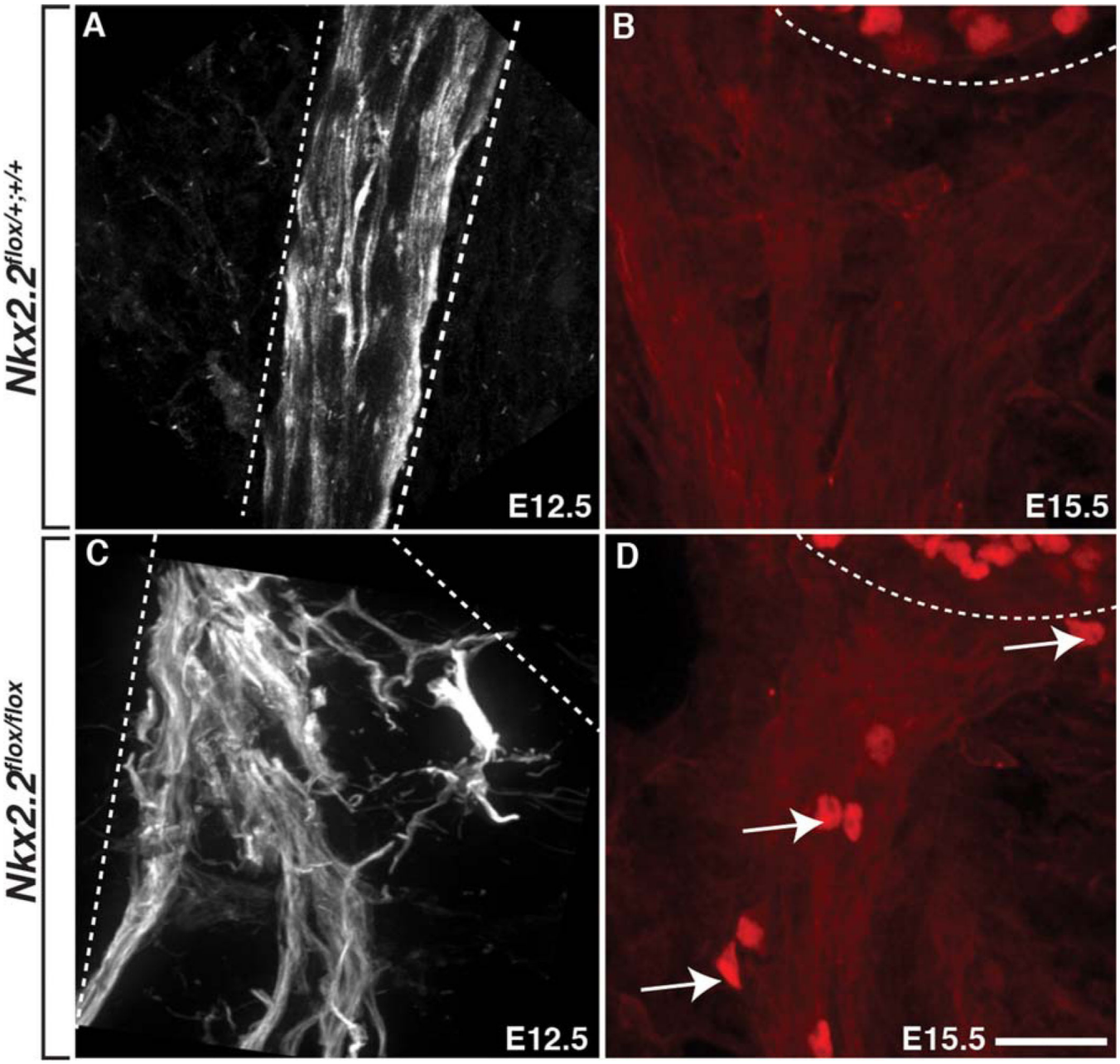

Fig. 5.

Nkx2.2^{+} perineurial glia are required for motor nerve development. **A:** At E12.5 in control embryos, tubulin^{+} axons exited the spinal cord in stereoptypical positions and were tightly fasciculated. **B**: At E15.5, Islet1/2^{+} motor neuron cell bodies were always restricted to the spinal cord in control embryos. **C:** In contrast, in *Nkx2.2$^{flox/flox}$* cKO mice, motor axons exited the spinal cord in ectopic positions and were severely defasciculated in the periphery at E12.5. **D:** Additionally, by E15.5, we observed Islet1/2^{+} motor neuron cell bodies (arrows) outside of the spinal cord ventral to the spinal cord (dashed line) in *Nkx2.2$^{flox/flox}$* cKO mice. Dashed lines denote outline of motor nerve and edge of ventral spinal cord. Scale bar = 25 μm.

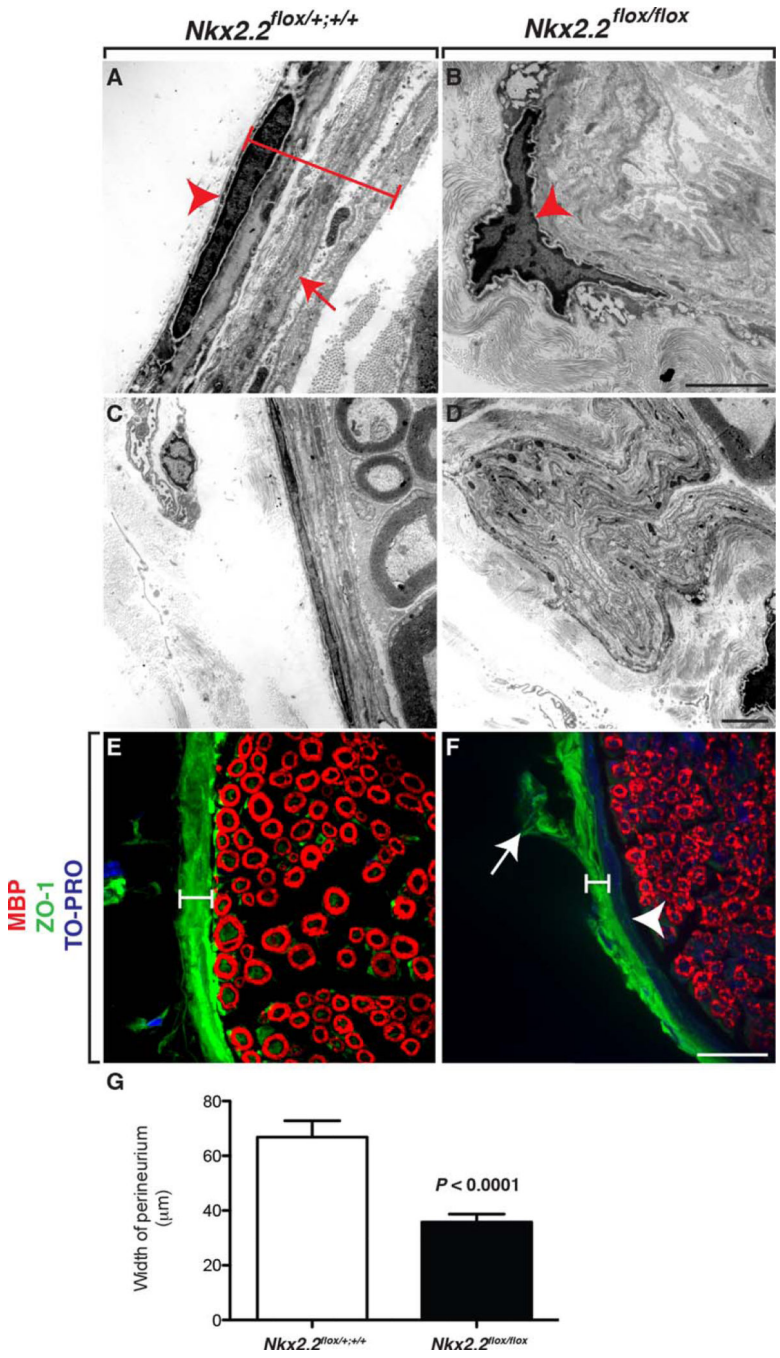

Fig. 6.

Loss of *Nkx2.2* perturbs perineurial development. **A:** In TEM images of control adult sciatic nerve, we observed several layers of elongated perineurial cells (bracket and arrowhead) with double basal lamina (arrow). **B:** In contrast, in *Nkx2.2*$^{flox/flox}$ cKO mice, perineurial layers were highly disorganized and cells were more rounded (arrowhead). **C,D:** Additionally, in contrast to control littermates, which had a smooth and even layer around the entire perimeter of the nerve, the perineurium in *Nkx2.2*$^{flox/flox}$ cKO sciatic nerves did not evenly encase the nerve and formed out-pockets of perineruial cells. **E:** In control adult

sciatic nerves labeled with antibodies specific to MBP and ZO-1, high levels of tight junctions were observed within the perineurium (bracket). **F:** In mice lacking *Nkx2.2*, the perineurium was disorganized (arrow) and ZO-1 labeling was much thinner (bracket). However, the inner perineurial epithelium was present as evidenced by TO-PRO^{+} nuclei (arrowhead). **G:** Graphical representation of the quantification of perineurial thickness measured by ZO-1 labeling. Black scale bar = 200 nm; white scale bar = 25 μm.

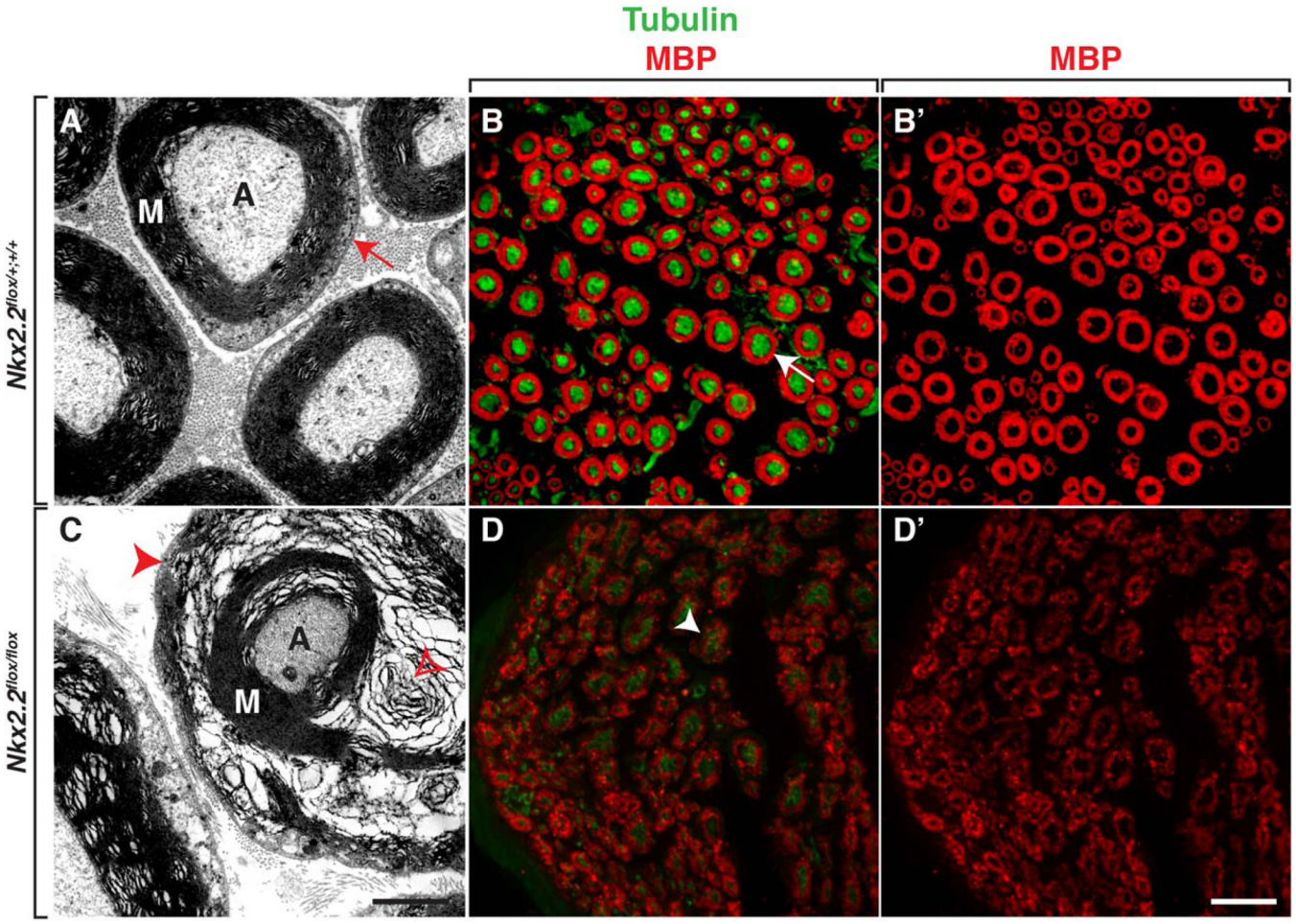

Fig. 7.

Aberrant perineurial differentiation perturbs Schwann cell differentiation. **A:** In transverse sections of control adult sciatic nerves, TEM shows that Schwann cells differentiate and make compact myelin around large diameter axons (red arrow). **B,B':** Antibody labeling of control sciatic nerves with MBP and tubulin confirm that myelin is compact (arrow). **C:** In contrast, in sciatic nerves harvested *Nkx2.2*$^{flox/flox}$ cKO mice, TEM demonstrates that although Schwann cells make myelin, it is highly disorganized and not compact (red arrowhead). Additionally, we often observed "spirals" of myelin (open red arrowhead) around axons in *Nkx2.2*$^{flox/flox}$ cKO nerves. **D,D':** MBP and tubulin labeling of *Nkx2.2*$^{flox/flox}$ cKO sciatic nerves confirm this perturbed myelin (arrowhead) phenotype. M, myelin; A, axon. Black scale bar = 200 nm; white scale bar = 25 μm.

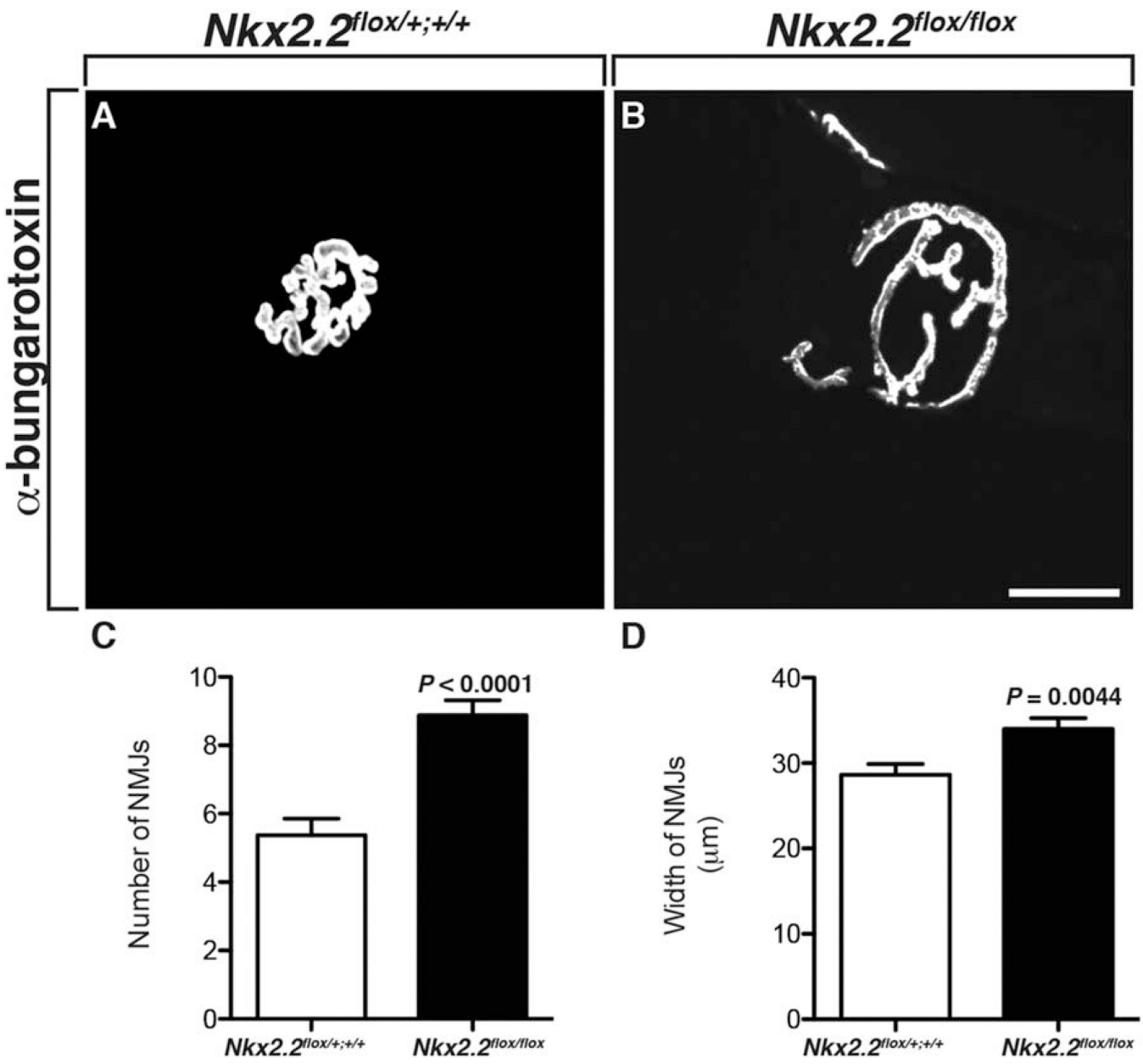

Fig. 8.

NMJ maturation is defective with loss of *Nkx2.2* **A:** In adult wild-type mice, somatic muscle sections labeled with an antibody to α-bungarotoxin showed mature NMJs. B: In muscle harvested from adult *Nkx2.2*$^{flox/flox}$ cKO mice, α-bungarotoxin labeling revealed that NMJs were larger. **C,D:** Quantification of both the number and size of NMJs in adult somatic muscle demonstrated that there were significantly more α-bungarotoxin^{+} NMJs and that they were larger in mice lacking *Nkx2.2*. Scale bar = 25 μm.